Analyze of Impedance for Water Management in Proton Exchange Membrane Fuel Cells Using Factorial Design of (DoE) Methodology

Khaled. Mammar[1], Abdelkader. Chaker[2]
1- Departement of Electrical and Computer Engineering, University of Bechar, Algeria.
Email: mammar.univ.dz@gmail.com
2- Department of Computers and Informatics, Faculty of Electrical Engineering and Informatics
, Laboratory of Electrical network, E.N.S.E.T, B.P 1742 El M'naouar, Oran, Algeria
Email: chakeraa@yahoo.fr

Received: November 2012 Revised: April 2013 Accepted: May 2013

ABSTRACT:
Electrochemical impedance spectroscopy (EIS) is a very powerful tool for exploitation as a rich source of Proton Exchange Membrane Fuel Cell (PEMFC) diagnostic information.
A primary goal of this work is to develop a suitable PEMFC impedance model, which can be used to analyze flooding and drying of the fuel cell. For this one a novel optimization method based on Factorial Design methodology is used. It was applied to parametric analysis of electrochemical impedance Thus it is possible to evaluate the relative importance of each parameter to the simulation accuracy. Furthermore this work presents an analysis of the PEMFC impedance behavior in the case of flooding and drying

KEYWORDS: PEMFC fuel cell; Electrochemical Impedance Spectroscopy (EIS); Water management; Design of Experimental (DoE); Fractional factorial design.

1. INTRODUCTION

In the recent years because of the energy shortage and environmental concerns, renewable and clean energy become more and more popular. One of the alternative sources of the electric power is fuel cell. It is the clean energy, without any harmful emissions to the environment and has high power density. Proton Exchange Membrane (PEM) fuel cell is one kind of the fuel cells that can work in a comparatively high efficiency and low temperature condition. It is one of the promising technologies for alternative power source of residential power generation in the future [1]-[5].

A PEMFC converts the chemical energy of a fuel, just as the hydrogen H_2 and an oxidizer, just as the oxygen O_2 to electrical energy. The outline of a typical PEMFC is illustrated in Fig. 1 [2]. On one side of the cell, referred to as the anode, the fuel is supplied under certain pressure. The fuel for this model is the pure gas H_2, although other gas compositions can be used. In these cases, the hydrogen concentration should be determined in the mixture. The fuel spreads through the electrode until it reaches the catalytic layer of the anode where it reacts to form protons and electrons, as shown below in the reaction given in Eq. (1) [1]-[5]:

$$H_2 + 1/2\ O_2 \rightarrow H_2O + \text{heat} + \text{electrical energy} \quad (1)$$

In order to get an electric current out of this reaction, hydrogen oxidation and oxygen reduction are separated by a membrane, which is conducting protons from the anode to the cathode side. The semi reactions on both electrodes are

$$H_2 \rightarrow 2\,H^+ + 2\,e^- \quad \text{anode} \quad (2)$$

$$O_2 + 4\,e^- \rightarrow 2\,O^{2-} \quad \text{cathode} \quad (3)$$

While the protons are transported through the membrane, electrons are carried by an electric circuit along which their energy can be used. This process is shown in Fig.1.

Protons are able to cross the membrane only if attached to water molecules. Thus, it is of the prime importance to ensure at all the time that there is the minimum steady water content in the electrolyte. Water management is one of the most critical elements of PEM fuel cell design [6].

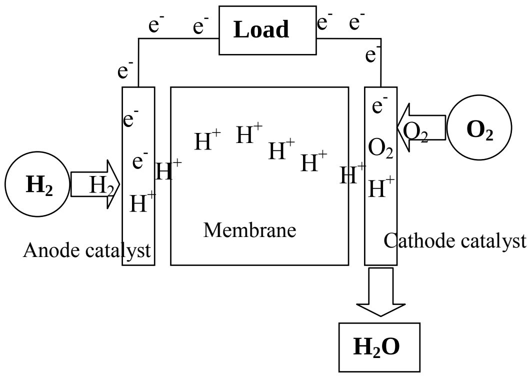

Fig. 1. Basic Fell Cell Operation.

Water molecules can enter the PEMFC via the anode and cathode gas streams. They are produced at the cathode by the oxygen reduction.H2O primarily evaporates at the cathode exits from the PEMFC. In the main order this paper outlines the processing and results of algorithm development for fuel cell diagnostics using electrochemical impedance spectroscopy (EIS) data [6]-[8]. This has been done to assist with the development of both onboard and off-board fuel cell diagnostic hardware. Impedance can identify faults that cannot be identified solely by a drop in cell voltage. Furthermore, it is able to conclusively identify electrode/flow channel flooding and membrane drying.

2. IMPEDANCE FUEL CELL MODEL FORMULATION

When there is no mass transport limitation, the redox reaction is simply represented by an equivalent electrical circuit of parallel RC cells. However, when there are considerable variations of the interfacial concentrations on electrodes, the Randles cell [6], is a common and practical way of modeling an electrochemical cell as an equivalent circuit. It consists of four elements: two resistors, *R*m, stands for the Ohmic resistance of the electrolyte, here the proton exchange membrane, and *R*p stands for the polarization resistance, due to the oxygen reduction reaction; a plane capacitor, *C*dl, represents the double layer capacitance at the electrode/electrolyte interface; and the impedance of diffusion called Warburg impedance. It was modeled by the equation from the Butler–Volmer equation and Fick's second law of diffusion; it is possible to derive the general expression of the diffusion impedance for a finite length diffusion layer, Z_W [6]:

$$Z_W(j.\omega) = \frac{RT}{n^2F^2S\sqrt{j\omega}} \frac{\tanh\sqrt{((j\omega)/D)\delta^2}}{C_o\sqrt{D}} \qquad (4)$$

Were:

δ : Diffusion layer width (m)

D: the diffusion coefficient ($m^2\ s^{-1}$)

N: number of electrons

R: perfect gas constant (J mol−1 K−1)

F: Faraday constant (A s mol−1)

C_o: oxygen concentration in cathode active layer (mol m−3)

S: active area (m2)

T: temperature (K)

Relation (1) can be re-written as:

$$Z_W(j.\omega) = \frac{RT}{n^2F^2S\sqrt{j\omega}} \frac{1}{C} \frac{1}{D} \delta \frac{\tanh\sqrt{(j\omega(\delta^2/D)}}{C\sqrt{\delta^2/D}} \qquad (5)$$

Which leads to the definition of two parameters, a time constant? τ_d

$$\tau_d = \frac{\delta^2}{D} \qquad (6)$$

and a resistance, R_d

$$R_d = \frac{RT}{n^2F^2S\sqrt{j\omega}} \frac{1}{C} \frac{1}{D} \delta \qquad (7)$$

This leads to the final expression of the concentration–diffusion impedance:

$$Z_W(j.\omega) = R_d \frac{\tanh\sqrt{(\tau_d.j.\omega)}}{\sqrt{(\tau_d.j.\omega)}} \qquad (8)$$

Were

R_d is dimensionally homogenous to an electrical resistance and τd is dimensionally homogenous to a time (s)

Finally, the total impedance of the fuel cell is composed of two impedances, one impedance for each electrode (anode and cathode), in series with the internal resistance R_m linked to the membrane. By making the further assumption that the rate limiting reaction is the oxygen reduction at the cathode, we will neglect the contribution of the anode impedance to the cell impedance. Thus, the equivalent circuit retained to model our fuel cell is that of Fig. 2, and the overall impedance is:

$$Z(j.\omega) = R_m + \frac{1}{j.\omega.C_d + (1/(R_p + Z_w))} \qquad (9)$$

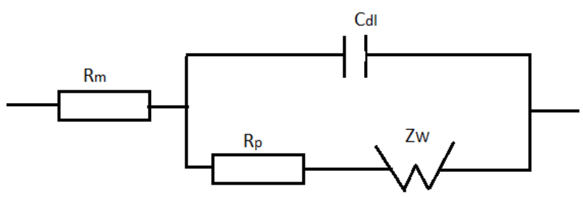

Fig. 2 Randles cell

As seen in Fig.3, the fitting of a Randles cell to the experimental data is good but not entirely satisfactory. The bulk of the problem comes from the high-frequency part of the model, for which the Randles cell predicts a semicircle center on the *x*-axis, while experimental data clearly show a depressed semicircle (i.e. centered below the *x*-axis). As a side-effect, the model misplaces the transition between the two semicircles. These depressed semicircles are usually dealt with by changing the standard plane capacitor of the Randles circuit into a constant phase element (CPE), as seen in Fig.3. Whereas the standard plane capacitor exhibits a first -order behavior, the CPE impedance is defined by:

$$Z_{CPE}(j.\omega) = \frac{1}{Q(j\omega)^{\alpha}} \quad (10)$$

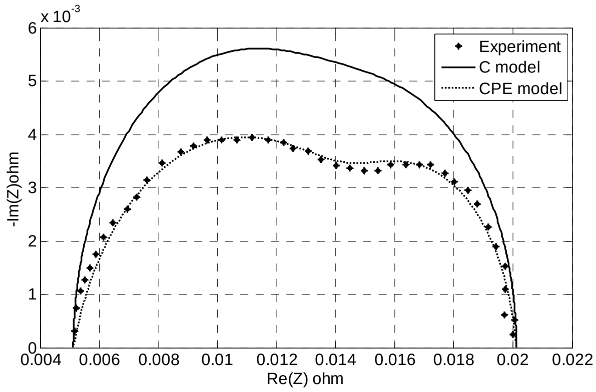

Fig. 3. Comparison between the experimental impedance data, a Randles cell model and a Randles cell model with a CPE

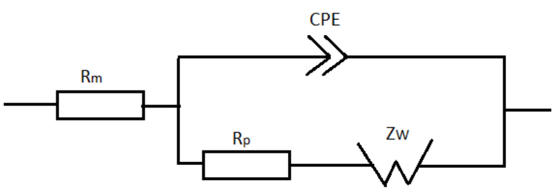

Fig. 4. Randles cell with CPE impedance.

With a value of α usually ranging between 0.5 and 1, the impedance of the equivalent circuit is now:

$$Z_T(j.\omega) = R_m + \frac{1}{Q(j.\omega)^{\alpha} + (1/(R_p + Z_{\omega}))} \quad (11)$$

For identification of model parameters the non-linear least square fitting algorithm of MATLAB® was used to identify the relevant parameters of Randles cell developed in Section 2. The principle of this algorithm is to minimize the square of a nonlinear function while finding the best values of the unknown Variable (i.e. model parameters) starting from their given initial values.

It should be noted that the impedance points measured at low frequencies, whose physical significance is not clear, and the points of impedance having a positive imaginary part (due to wiring inductance) are not taken into account for this identification process. As shown in Section 2, the parameters of the fractional model, which are to be identified, are R_m determined by an identification algorithm and then this value is used to do “fitting” for the other parameters of the model with experimental results. The value of the time constant τ_d is calculated from the frequency corresponding to the peak of the diffusion arc. As far as internal resistance R_m is concerned, it corresponds to the distance between the origin and the intersection of the impedance spectrum with the real axis.

The remaining parameters (R_d, R_p and Q) are identified by using non-linear least square algorithm. Table.1 shows the values of the model parameters identified for four impedance spectra Corresponding to flooding (RH=100%) and drying (RH=15%)

3. FACTORIAL DESIGN OF EXPERIMENTS METHODOLOGY

A Design of Experiment (DoE) is a structured, organized method for determining the relationship between a number of factors affecting a process and the output of that process. Regardless of the domain of application, this methodology is useful for three objectives: screening, optimization, and robustness testing. Employed at the beginning of the investigation of a new application, screening experiments are commonly designed to explore many factors, in order to evaluate their effects on the responses. It also makes it possible to obtain the best possible precision on the modeling of the results and thereafter the optimization of the process

3.1. Definition of variation intervals of the factors

In this study the Factorial Design methodology can be used to evaluate the respective impacts of the relative humidity RH (%) and Time t(s) on the FC impedance operation Table.1.

The full factorial design required 2^k +n experiments, where k is the number of factors [9]-[11]. The number of factors considered in our work are relative humidity RH (%) and Time t(s) the number of runs are 4 Table.2.

We use a full factorial design with 2 factors [9] .With such models, the response of the process is expressed according to the factors *ui (i = 1..., e)*:

$$y = f(u_i) = c_0 + \sum_{i=1..} c_i.u_i + \sum_{i \neq j=1..} c_{ij}.u_i.u_j \quad (12)$$

Table 1. Model parameters and cell voltage during the flooding and drying

Time(s)	RH(%)	Rm	Q	Rp	Rd	td	U
500	15	0,00512	0,952	0,0099	0,0051	0,1155	4,06
3700	15	0,0088	0,62	0,013	0,0101	0,1835	3,35
500	100	0,00398	1,109	0,008	0,0034	0,0872	4,18
3700	100	0,00416	0,936	0,0163	0,0312	0,0947	3,3

Wher c_0, c_i, and c_{ij} *are* calculated coefficients. A normalized centered value can be defined for each factor as follows:

$$x_i = \frac{(u_i - u_{ic})}{\Delta u_i} = u_i^* \tag{13}$$

Where:

$$u_{ic} = \frac{(u_{i\max} + u_{i\min})}{2} \quad \Delta u_{ic} = \frac{(u_{i\max} - u_{i\min})}{2} \tag{14}$$

With these notations, the function of the response becomes:

$$y = f(x_i) = a_0 + \sum_{i=1..} a_i x_i + \sum_{i \neq j=1..} a_{ij} x_i x_j \tag{15}$$

Where *xi* can obviously take only the values: −1 (for minimal input value x_{imin}), +1 (for maximal input value x_{imax}).

In the present study, i.e. x_1= t*(s), x_2=RH*(%), the linear model of impedance will take the following form:

$$\mathrm{Rm} = a_0^1 + a_1^1 t^* + a_2^1 \mathrm{RH}^* + a_{12}^1 t^* \mathrm{RH}^* \tag{16}$$

$$Q = a_0^2 + a_1^2 t^* + a_2^2 \mathrm{RH}^* + a_{12}^2 t^* \mathrm{RH}^* \tag{17}$$

$$R_P = a_0^3 + a_1^3 t^* + a_2^3 \mathrm{RH}^* + a_{12}^3 t^* \mathrm{RH}^* \tag{18}$$

$$R_d = a_0^4 + a_1^4 t^* + a_2^4 \mathrm{RH}^* + a_{12}^4 t^* \mathrm{RH}^* \tag{19}$$

$$\tau_d = a_0^5 + a_1^5 t^* + a_2^5 \mathrm{RH}^* + a_{12}^5 t^* \mathrm{RH}^* \tag{20}$$

$$U = a_0^6 + a_1^6 t^* + a_2^6 \mathrm{RH}^* + a_{12}^6 t^* \mathrm{RH}^* \tag{21}$$

Table 2. Matrix of full factorial design with two factors.

N	t^*	RH^*
1	-1	-1
2	1	-1
3	-1	1
4	1	1

The Matrix of full Factorial of such a design with two (t and RH) factors given in Table.1, developed by Software MODDE 5.0 (Umetrics AB, Umea, Sweden) allows creating and analyzes experimental designs; the program helps the user to analyze the results and predict the responses [9]-[11]. It calculates coefficients of the factors and allows modeling and optimizing the process. Obtained results according to the matrix are presented in Table.1 where the response of impedance parameters is obtained from the experimental manufactured by [5]. Furthermore, Fig.5 represents significant effect and interaction of the model parameters.

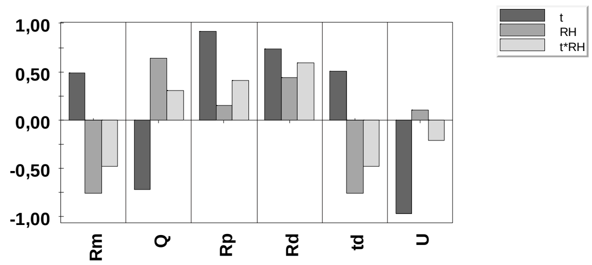

Fig.5. Plot coefficients of the effects and interactions factors of model parameters and cell voltage

The mathematical model of the response (Cell voltage) is linear with significant interactions, given by:

$$\mathrm{Rm} = 0{,}00609 + 0{,}00171949t^* \text{-} 0{,}00250279\mathrm{RH}^* \text{-} 0{,}00167439t^*\mathrm{RH}^* \tag{22}$$

$$Q = 0{,}90425 \text{-} 0{,}148901t^* + 0{,}1275\mathrm{RH}^* + 0{,}0667517t^*\mathrm{RH}^*$$

(23)

$$R_P = 0{,}0118 + 0{,}00334376t^* + 0{,}000557375\mathrm{RH}^* + 0{,}00150034t^*\mathrm{RH}^* \tag{24}$$

$$R_d = 0{,}01245 + 0{,}00944438t^* + 0{,}00553026\mathrm{RH}^* + 0{,}00770649t^*\mathrm{RH}^* \tag{25}$$

$$\tau_d = 0{,}120225 + 0{,}0221923t^* + \text{-}0{,}0326524\mathrm{RH}^* \text{-} 0{,}0219176t^*\mathrm{RH}^* \tag{26}$$

$$U = 3{,}7225 \text{-} 0{,}450102t^* + 0{,}0459784\mathrm{RH}^* \text{-} 0{,}0958537t^*\mathrm{RH}^* \tag{27}$$

3.2. Evaluation of the quality of the mathematical model

The quality of the obtained mathematical model can be evaluated by two statistical criteria which are given directly by software MODDE 5.0 to check experimental (*R*2 criterion) and predictive (*Q*2 criterion) quality of the mathematical model. When values of *R*2 and *Q*2 are close to the unit, the model is considered as good and can be used for optimization and prediction [11]. As values of these two criteria, according to the model given by equation (15), are respectively $R2 = 0.999$ and $Q2 = 0.943$ the model can thus be used to predict and optimize the process.

4. SIMULATION RESULTS AND DISCUSSION OF THE IMPEDANCE RESPONSE

We simulate progressive behaviour of impedance with variation in time from (500 to 2700) under dehydrating conditions RH=10% (e.g., dry gas feeds). Bode plots of spectra from dehydrated PEMFCs are characterized by an increase of cell impedance magnitude across all frequencies and an increase (less capacitive) in phase angle at the mid to high frequencies fig(6). The dehydration effect is equally visible in the Nyquist plot Fig .7 which shows a right lateral shift by the amount of the membrane resistance (R_{int}) increase

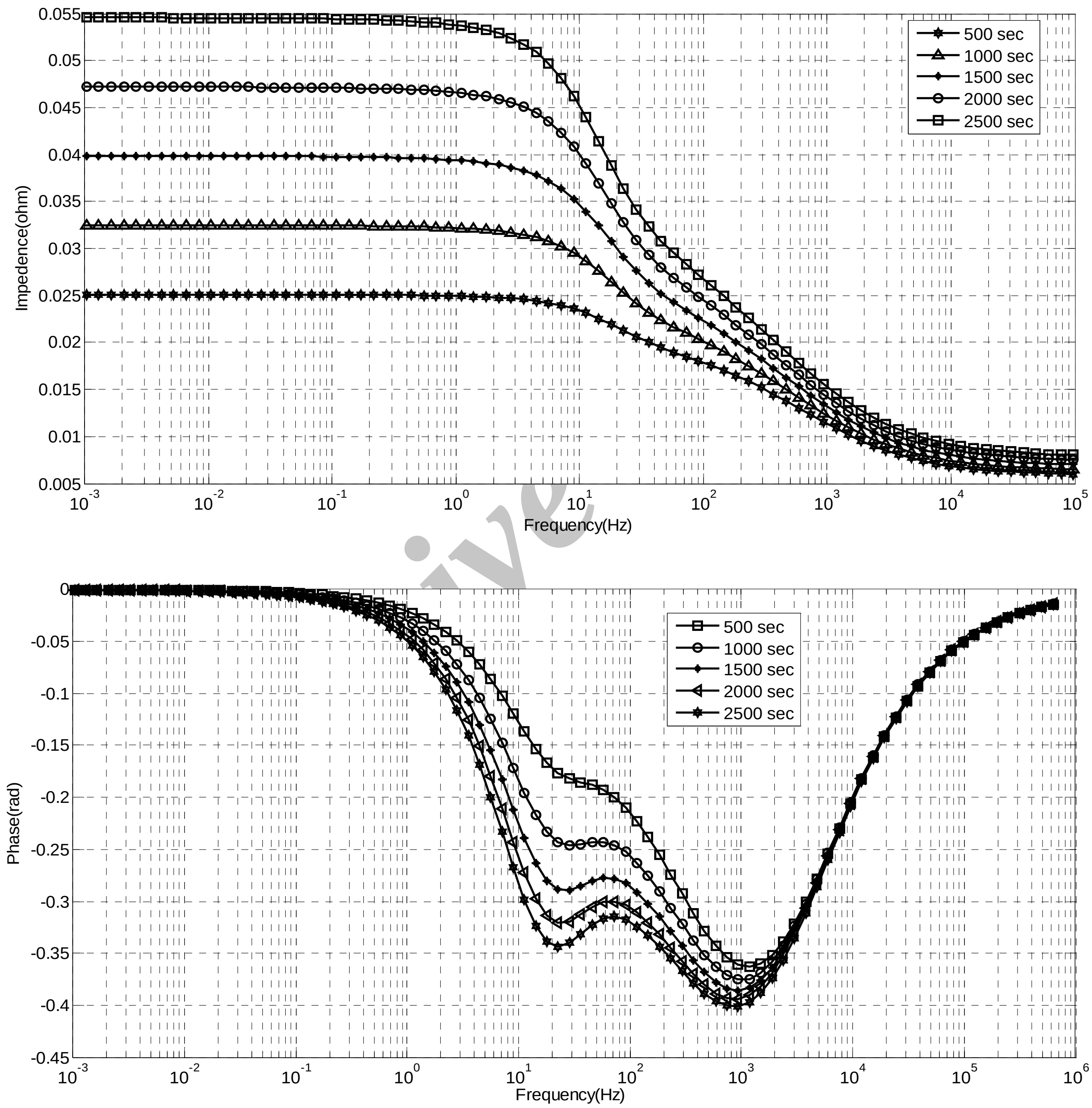

Fig. 6. Effect of dehydration on PEMFC: Bode plot (normal t=500sec→dehydrated t=2700 sec)

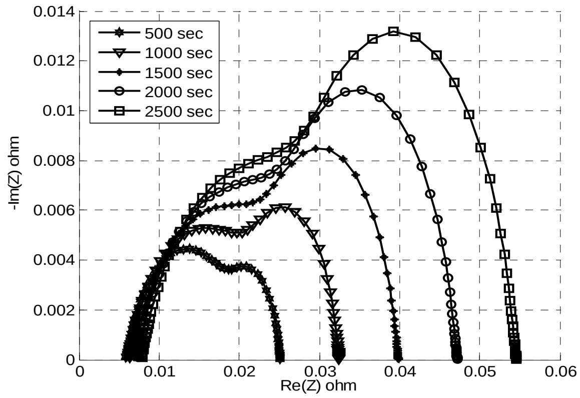

Fig.7.Effect of dehydration on PEMFC: Nyquist plot (normal t=500sec→dehydrated t=2700 sec)

Under high load conditions, fuel cell current density increases and the production of water at the cathode increase by oxygen reduction reaction (2) and electro-osmotic drag . Unchecked, this can lead to flooding case. The initial stage of flooding is characterized by a slow decrease in output voltage as liquid water begins to accumulate in the channels and constrict the gas flow, thus increasing the diffusion related equivalent circuit parameters R_d and time constant τ_d . We simulate progressive behaviour of impedance with variation in time from (500 to 2700) under flooding conditions RH=150%. Bode plots of spectra from flooding PEMFCs are characterized by an increase of low frequency cell impedance magnitude and a decrease in phase angle (more capacitive) at the mid to low frequencies fig(8).

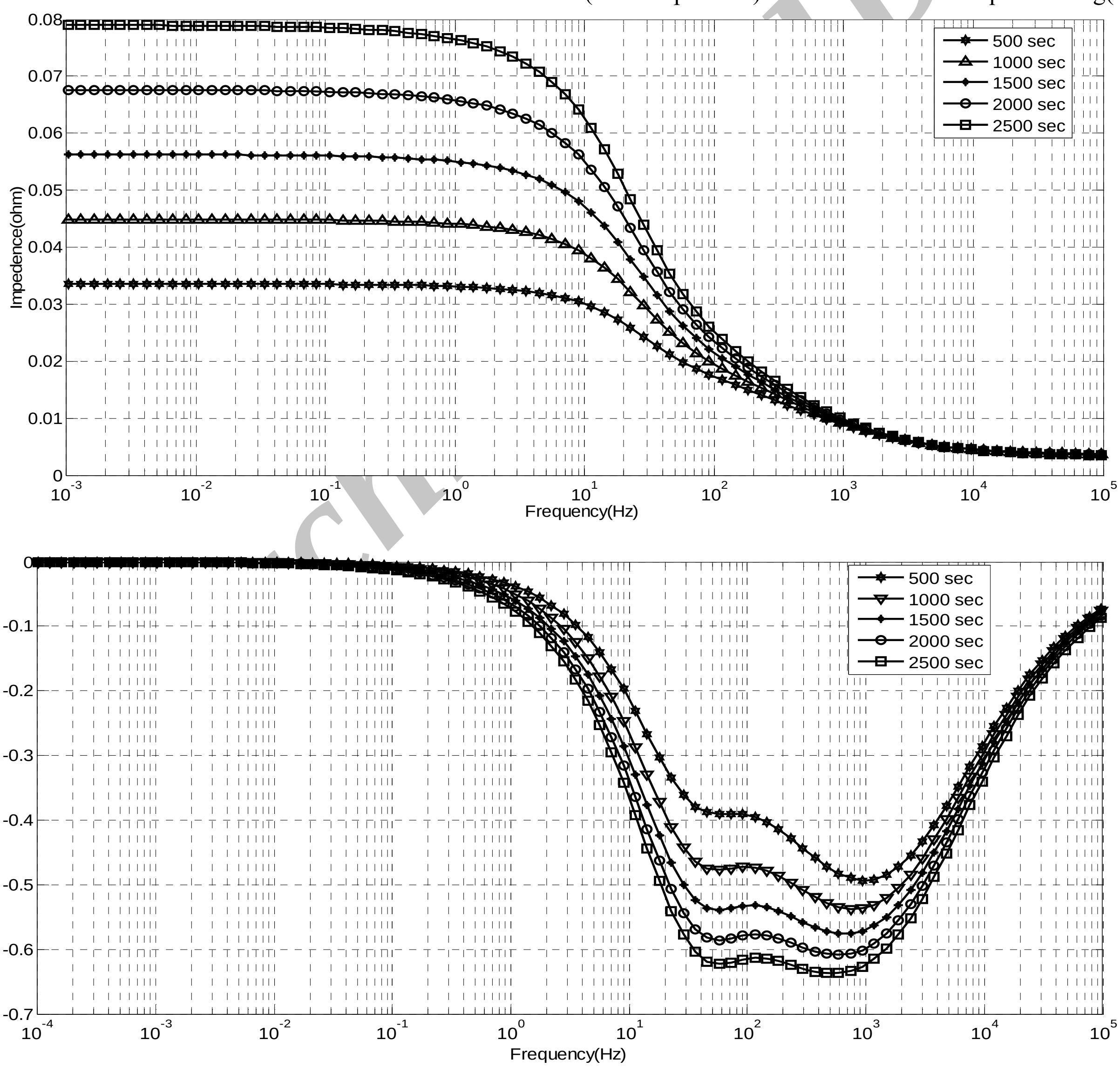

Fig. 8. Effect of flooding on PEMFC: Bode plot (normal t=500sec→flooded t=2700 sec)

The flooding effect can be related to the equivalent circuit parameter changes in the Nyquist plot Fig.9 which the absence of large variations in the high-frequency arcs. This behavior can be explained , noting that the humidification levels in the membrane (and consequently the membrane resistance) do not change between normal and flooded conditions (i.e., the membrane is fully humidified in both cases).

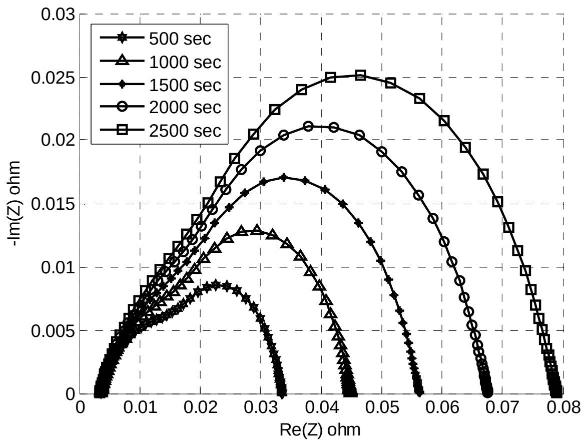

Fig. 9. Effect of flooding on PEMFC: Nyquist plot (normal t=500sec→ flooded t=2700 sec).

In main order to make the diagnosis of flooding and drying we simulate progressive behaviour of impedance with time (500 to 2700) and the relative humidity RH (%) from(10% to 100%) and make a diagnosis-clogging a fuel cell using the 5 criteria behavior on the impedance:

1-Internal resistors R_{int} (measured at high frequency)
2-biasing resistors R_{pol} (measured at low frequency)
3 frequency of arc-Summit f_{max}
4- Imaginary of arc summit I_{max}
5-area (Re(Z)*Im(Z))

As shown in Fig.10 the value of the resistance measured at high frequency of the stack R_{int} increases with time acutely when RH% of cathode reactant gas decreases from 100% to 20%. The main reason is the conductivity of the membrane in a PEMFC directly related to its water content. When RH% increases, the water content in membrane will increase, consequently the membrane conductivity will increase and the R_m of the stack will decrease.

The resistance measured at low frequency of the stack R_{pol} is shown in Fig.11, it gradually increases according to the time as RH % of the cathode reactant gas increases. Because the relative humidity (RH %) affects the proton mobility at high frequency.

Fig. 12 shows the frequency of arc –summit f_{max} behavior. It emphasizes this observation that the arc –summit frequency stays constant with variation of the relative humidity RH % and time.

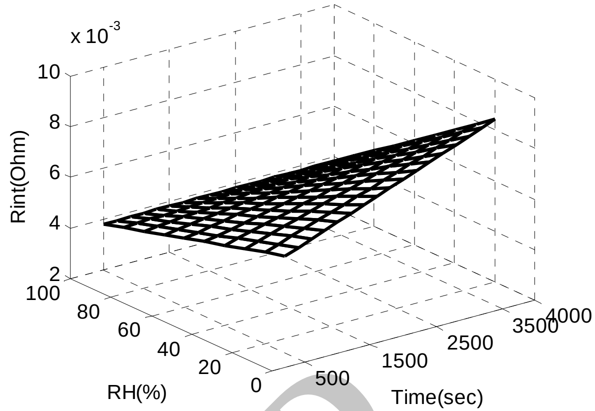

Fig. 10. Internal resistors R_{int} behavior

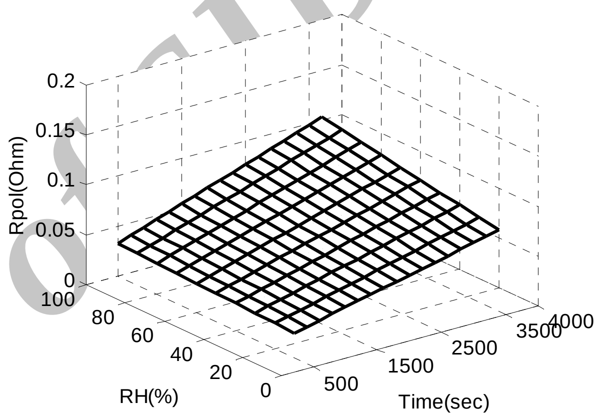

Fig. 12. Resistance at low frequency of the stack R_{pol}

As shown in Fig. 13 and Fig.14, the value of imaginary of arc summit Imax and area(Re(Z)*Im(Z)) increase with time acutely when RH% of cathode reactant gas increases from 100% to 20%. The main reason is the conductivity of the membrane in a PEMFC directly related to its water content. When RH increases, the water content in membrane will increase, consequently the membrane conductivity will increase and the R_m of the stack will decrease.

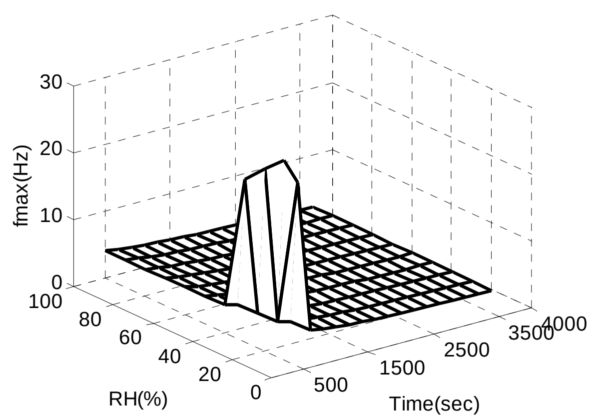

Fig. 12. Arc –summit f_{max} behavior

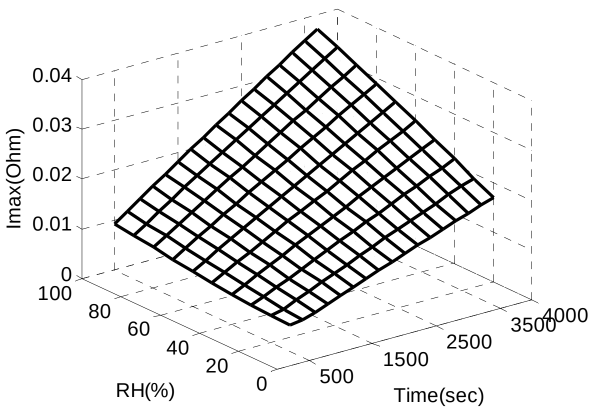

Fig. 13. Imaginary of arc summit I max behavior

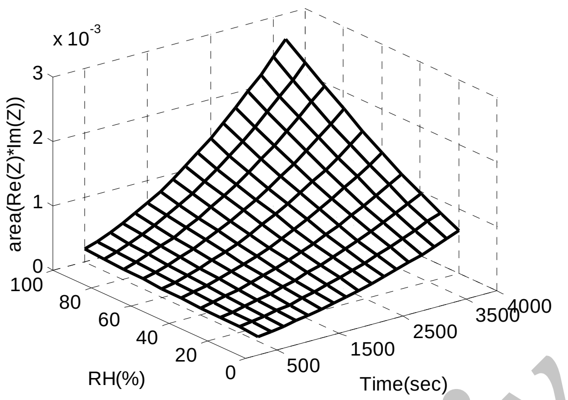

Fig. 14. Area (Re(Z)*Im(Z)) behavior

5. CONCLUSION

The technique of the electrochemical impedance spectroscopy EIS was demonstrated as a powerful tool in order to diagnose the Proton Exchange Membrane Fuel Cell (PEMFC) behavior in the case of flooding and drying. This paper proposes a simple impedance model represented by an equivalent electrical circuit called Randles. This model augmented with a CPE was found to be an accurate model of the fuel cell's electrical response over a wide range of operating conditions. Furthermore Factorial Design Methodology (DoE) method has been used to evaluate the respective impacts of the relative humidity RH (%) and Time t(s) on the FC impedance operation. This new approach allowed us to identify a set of two parameters exhibiting high sensitivity to either flooding or drying out of the membrane electrode assembly. Robust and reliable PEM fuel cell's state of hydration monitoring was demonstrated using the resistance measured at high frequency of the stack R_{int} and the resistance measured at low frequency of the stack R_{pol}. However, a further study is necessary to develop a more specific algorithm for the simulation of the transient response. The major work needed in the future consists of defining more systematic methods for identification of the parameters and their validation particularly in the time domain. Moreover, it would also be interesting to use the Fuzzy Logic FLC controller for water management based on the measured resistance at high frequency of the stack R_{int} and the measured resistance at low frequency of the stack R_{pol}.

REFERENCES

[1] JEFERSO JEFERSON M. Corrêa, Student Member, IEEE, Felix A. Farret, Luciane N. Canha, and Marcelo G. Simões **"An Electrochemical-Based Fuel-Cell Model Suitable for Electrical Engineering Automation Approach"**, *IEEE Transactios on Industrial Electronics,* Vol. 51, No. 5, Octobr 2004.

[2] G. Naga Srinivasulu, T. Subrahmanyam and V. Dharma Rao: **"Parametric sensitivity analysis of PEM fuel cell electrochemical Model"**, International Journal of Hydrogen Energy, Science Direct, article in press I-7, 2011.

[3] Kh. Mammar and A. Chaker, **" Fuzzy Logic Control of Fuel Cell System for Residential Power Generation"**, *Journal ,of ELECTRICAL ENGINEERING,* Vol. 60, No. 6, pp. 328–334, 2009.

[4] Kh. Mammar, A. Tahour and A. Chaker, **"Active and Reactive Power Control of Fuel Cell System Using a Neural Network Model and Fuzzy Logic Controller",** *International Review of Automatic Control (Theory and Applications)*, May. 2010.

[5] M. T. Outeiro, R. Chibante, A. S. Carvalhoc,d, A. T. de Almeida **"A parameter optimized model of a Proton Exchange Membrane fuel cell including temperature effects"**, *Journal of Power Sources 185*, pp. 952–960, 2008.

[6] N. Fouquet, C. Doulet, C. Nouillant, G. Dauphin-Tanguy and B. Ould-Bouamama **"Model based PEM fuel cell state-of-health monitoring via ac impedance measurements",** *Journal of Power Sources 159*, pp. 905–913, 2006.

[7] M. A. Danzer and E. P. Hofer, **"Analysis of the electrochemical behaviour of polymer electrolyte fuel cells using simple impedance models",** *Journal of Power Sources 190*, pp. 25–33, 2009.

[8] J. R. Macdonald and W. B. Johnson**, "Impdedance Spectroscopy: Theory, Experiment and Applications"**, *John Wiley & Sons,* pp. 1–26, 2005.

[9] L. Eriksson, E. Johansson, N. Kettaneh-Wold, C. Wikstöm, and S. Wold, **"Design of Experiments, Principles and Applications"**, Umetrics, 2009

[10] C. R. Hicks and K. V. Turner, Jr., **"Fundamental Concepts in the Design of Experiments",** *Oxford, U.K.: Oxford Univ. Press,* 1990

[11] T. P. Ryan, G. A. Acworth, **"Modern Experimental Design",** by John Wiley & Sons, Inc. All rights reserved 2007.